Role of magnetic impurities in Fe/V multilayers

B. Skubic,[1] E. Holmström,[2,3] A. Bergman,[1] and O. Eriksson[1]
[1]*Department of Physics, Uppsala University, Box 530, SE-751 21 Uppsala, Sweden*
[2]*Instituto de Física, Universidad Austral de Chile, Valdivia, Chile*
[3]*Theoretical Division, Los Alamos National Laboratory, Los Alamos, New Mexico 87545, USA*
(Received 21 August 2007; revised manuscript received 18 February 2008; published 4 April 2008)

We have studied the Fe/V bcc (100) multilayers and the effect of alloying the V spacer layers with various amounts of magnetic impurities (Fe, Co, Ni, and Cr). The study was performed by means of total energy electronic structure calculations. We compare the effect of the different types of impurities and discuss the interlayer exchange coupling in terms of Fermi surface topology and bulk magnetic order. The effect of interface roughness and interface intermixing on the phase diagrams was also studied.

DOI: 10.1103/PhysRevB.77.144408 PACS number(s): 73.61.At, 75.70.Cn, 75.75.+a, 85.75.Ss

I. INTRODUCTION

There has been a large amount of research on multilayers of alternating magnetic and nonmagnetic layers published during the past years. These materials have found important applications in hard disk reading heads and magnetic sensors.[1–3] Two important properties of these materials, which are the oscillating interlayer exchange coupling (IEC) and the giant magnetoresistance, i.e., a drastic modification in the resistance as a function of an applied field, greatly influence the function of these multilayers as magnetic sensors. The Ruderman–Kittel–Kasuya–Yosida (RKKY) coupling was identified as the mechanism behind the IEC. Although the interlayer coupling in multilayers is considered to be relatively well understood, multilayers with slightly magnetic spacer layers have not been thoroughly studied before. It has been seen that by introducing a small amount of a magnetic impurity in the spacer layers, one can open up a channel for a direct exchange between the magnetic layers, which may be used as a method of tuning the IEC.[4] The influence of impurities in the spacer on the IEC layers may also be important for understanding multilayers with poor interfaces, where a portion of the magnetic atoms has diffused into the spacer layers.

In this paper, we present an investigation of the coupling mechanism in Fe/V multilayers with different kinds of magnetic impurities in the V spacer layers. The Fe/V system has been thoroughly studied both experimentally and theoretically in previous work.[5] Here, we present *ab initio* electronic structure calculations on Fe/V with different impurities, such as Cr, Fe, Co, and Ni in the V spacer layer. We present the phase diagrams for a range of spacer thicknesses and impurity concentrations and discuss the physical mechanisms behind the details of the phase diagrams.

II. THEORY

A. Calculation method

The IEC, here defined as the energy difference between the antiferromagnetic (AFM) and the ferromagnetic (FM) configuration, $J=E_{\mathrm{AFM}}-E_{\mathrm{FM}}$, was obtained by total energy calculations. These first principles self-consistent electronic structure calculations were performed by means of a spin-polarized interface Green function technique, which is based on the linear muffin-tin orbital method within the tight-binding, frozen core, and atomic sphere approximations. The method was developed by Skriver and Rosengaard.[6] Furthermore, we have used the local spin-density approximation as parametrized by Perdew *et al.*[7] and the principal layer technique.[8] The alloys were treated within the coherent potential approximation (CPA).[9–11] Calculations were converged both in total energy and with respect to k-space sampling. The use of 528 k-points in the irreducible Brillouin zone was sufficient to obtain convergence in all considered cases. Calculations were done for a bcc structure of the whole multilayer structure in the experimental volume of vanadium.

B. Interlayer exchange coupling

The interlayer coupling determines the magnetic phase diagram of a multilayer. For the Fe/V system with impurities, the phase diagram consists of two different regions and a transition zone between the regions. The two regions will be referred to as the low impurity and high impurity regions. In the low impurity region, the spacer is nonmagnetic and the coupling is given by a RKKY-type coupling, which largely depends on the Fermi surface of the spacer and of the reflection coefficients at the multilayer interfaces. In the high impurity region, the spacer is magnetic and the coupling between the Fe layers is governed by a direct exchange interaction through the magnetic spacer. A transition zone appears at the onset of magnetism in the spacer.

1. Direct exchange

The onset of magnetism in the spacer can roughly be understood in terms of the bulk properties of the spacer material. In Fig. 1, we plot the calculated bulk magnetization for the alloys FeV, CoV, and NiV. All calculations were done for the bcc structure in the volume of vanadium. Calculations were performed on a unit cell consisting of one CPA atom. This constricts a possible magnetic ordering to a ferromagnetic ordering. For some alloys and alloy concentrations, we can expect more complex magnetic ordering such as AFM order or a spin-density wave (SDW). These magnetic structures are not captured in our simple bulk calculations. As an

 ©2008 The American Physical Society

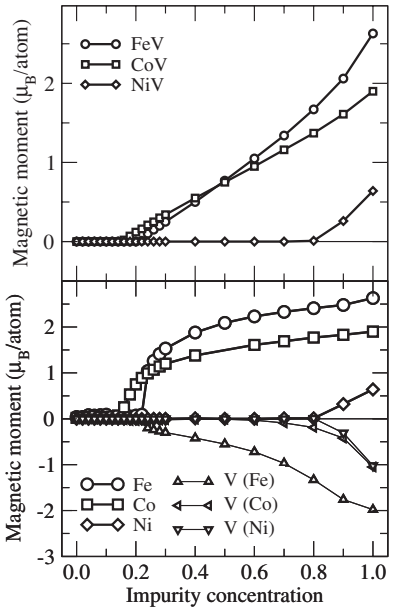

FIG. 1. Magnetization of bcc bulk alloys of V with Fe, Co, and Ni. The upper panel shows the average magnetization and the lower panel shows the individual V and impurity moments.

example, the alloy CrV shows no average magnetic moment or magnetic moment of the individual alloy components in our bulk calculations, but is expected to have a SDW. In multilayer calculations where the constriction on the magnetic order is partially relieved, we find indications of a SDW for certain alloy compositions of CrV and CoV. For the bulk alloys presented in Fig. 1, an onset of magnetism appears at some impurity concentrations and we may expect a similar onset in the spacer layer. Differences between the magnetic order of bulk and spacer layers are due to finite size effects and interface effects, such as interface hybridization, interface intermixing, and interface roughness. The influence of the interface quality on the spacer will be discussed in Sec. III A 2.

2. Ruderman–Kittel–Kasuya–Yosida coupling

A general expression for the asymptotic form of an interlayer exchange coupling through a nonmagnetic spacer was presented by Stiles[12] and Bruno.[13] The bilinear term can be written as

$$J = E_{\mathrm{AFM}} - E_{\mathrm{FM}} = -\sum_{\alpha} \frac{J_{\alpha}}{N^2} \sin(q_{\perp}^{\alpha} N + \phi_{\alpha}), \tag{1}$$

where N is the spacer thickness and the sum is over critical spanning vectors $q_{\perp}^{\alpha}$ of the bulk Fermi surface of the spacer material. The amplitude J_{α} of the coupling period α depends on the spin asymmetry of the reflection coefficients at the interfaces for corresponding $k_{\parallel}$. It also depends on the Fermi velocity and the curvature of the Fermi surface at the Fermi surface points spanned by $q_{\perp}^{\alpha}$. The phase of the coupling, ϕ_{α}, depends on both the reflection coefficients and the Fermi surface topology. Hence, the coupling is characterized by a set of superimposed oscillations where the periods are given by the extremal Fermi surface calipers.

As impurities are introduced in the spacer, the IEC is modified in several ways. The Fermi surface is modified by changing the length of the Fermi surface calipers responsible for the coupling. The interface reflection is modified by changing the amplitude and the phase of the oscillation periods. Finally, impurities introduce disorder into the spacer, leading to disorder scattering, which results in an additional damping factor to the coupling.[14–16] The expression for the IEC for the case of alloying is

$$J = -\sum_{\alpha} \frac{J_{\alpha} e^{-N/\Lambda}}{N^2} \sin(q_{\perp}^{\alpha} N + \phi_{\alpha}), \tag{2}$$

where the characteristic length Λ is given by

$$\frac{1}{\Lambda} = \frac{1}{\lambda^{+}} - \frac{1}{\lambda^{-}}, \tag{3}$$

where $\lambda^{+(-)}$ are mean free paths in the out of plane direction at the two Fermi surface points connected by the spanning caliper responsible for the oscillation.

C. Interface alloying

The concentration profile around each interface due to intermixing is modeled by a general normal cumulative distribution function with standard deviation Γ_C. The distribution is assumed to be equal at all interfaces.

This approach is a simplification, since the inherent surface diffusion of the elements is strongly dependent on the material combination and order, growth environment, and sample history. However, this assumption does not hamper a quantitative analysis, since the major influence on the magnetic properties does not depend on which of the interfaces the alloying takes place; the exchange coupling is acting over a large surface area and may be expected to average out local nonsymmetric alloying.

The concentration profile of the multilayer is then obtained as a sum over the interfaces in the sample, and the expression for the wavelike multilayer concentration profile is

$$C(X,\Gamma_C) = \sum_{i \neq 0} -1^{(|i|+1)} \Lambda_i(\mathrm{sgn}(i)X,\Gamma_C), \tag{4}$$

where Λ_i is the distribution function centered at interface i. The sum should be performed over all interfaces of the system. By taking, for example, interface $i=1$ as $X=0$ and counting layers from this interface, we obtain the layer concentration at layer N as $C(N-0.5,\Gamma_C)$, where the 0.5 term comes from the fact that the interfaces are located in between the atomic layers. Once the concentration profile is obtained, the interlayer exchange coupling and the total magnetic moment of a multilayer with interface intermixing may be calculated directly by means of our first principles method.

III. RESULTS

In Fig. 2, we show the calculated phase diagrams of $\mathrm{Fe/V}_{1-x}T_x\mathrm{/Fe}$ multilayers with impurities T=Fe, Co, Ni, and Cr for $0.3 \geq x \geq 0$. The white areas display AFM regions,

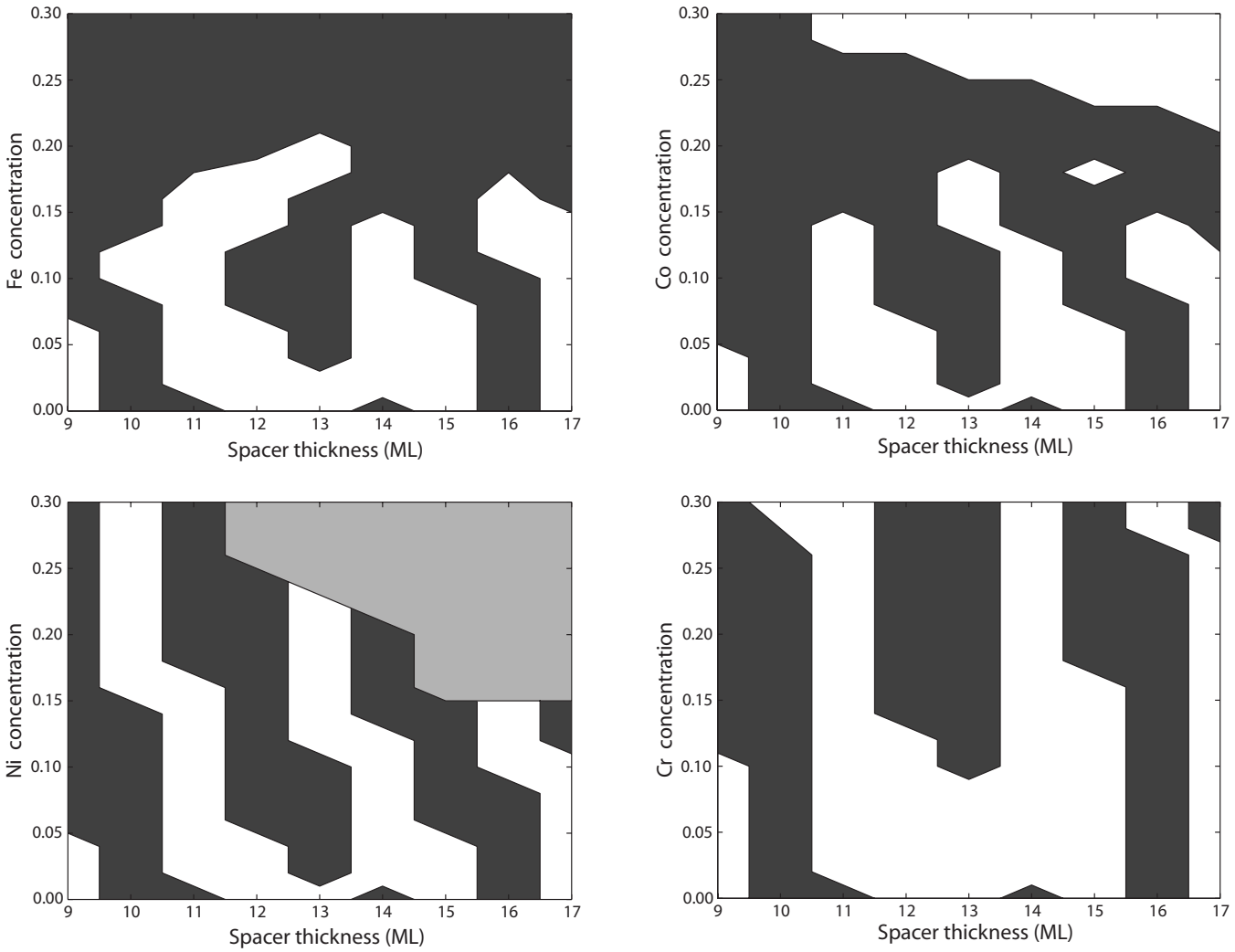

FIG. 2. Phase diagram for $Fe_3/[T_xV_{1-x}]_n$ multilayers where T=Fe, Co, Ni, or Cr. The horizontal axis shows the spacer thicknesses n and the vertical axis shows the impurity concentration x in the spacers. Black regions represent FM ordering and white regions represent AFM ordering. The gray region in the phase diagram for Ni impurities represents a region where the coupling strength is <2 μRy.

whereas the dark areas display FM regions. For the case of Fe impurities, the coupling changes from oscillating for small impurity concentrations to completely FM for Fe concentrations above 20%. For the case of Co impurities, the situation is similar with the exception of an AFM region opening up for large spacer thicknesses and high impurity concentrations. The AFM region is created due to the appearance of a spin-density wave within the CoV layer in the high concentration region. For Ni and Cr impurities in the spacer, there is no switch from an oscillating IEC to a constant coupling. Instead, a more complex phase diagram emerges. In the following sections, we will discuss in more detail the phase diagrams and how the different regions are affected by the alloying.

A. Ruderman–Kittel–Kasuya–Yosida region

1. Fermi surface change

Although Fe/V systems have been experimentally and theoretically studied, it is not well known which Fermi surface calipers are responsible for the oscillations in the IEC. Previous electronic structure calculations indicate a short period oscillation and a long period oscillation. In Ref. 17, these were found to be 3 and 11 ML long, while in Ref. 18, for $Fe_{0.82}Ni_{0.18}$/V (001) multilayers, a similar system, with periods of approximately 3 and 18 ML, were seen. The experiments on Fe/V (001) multilayers[19,20] are consistent with a long period oscillation of 10–20 ML. Interface roughness and interface intermixing are found to be responsible for the loss of the short oscillation period in the experiments.

From our calculations on Fe/V for the considered spacer thickness range, one may extract the coupling periods by performing a Fourier transform of N^2J. The considered spacer thickness range is in the preasymptotic region, which limits a comparison to asymptotic models for the IEC.

We anyhow find that the transformation has peaks corresponding to coupling periods of 2, 2.8, and 4.8 ML (data not shown). In addition, there is clearly a long period oscillation that is not caught by the Fourier transform since it is beyond the investigated thickness range. By analyzing the Fermi sur-

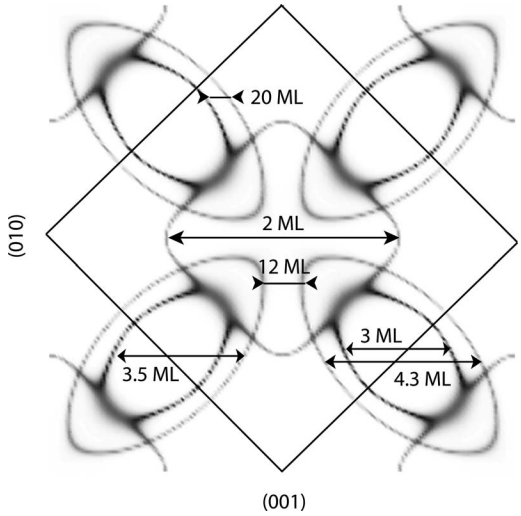

FIG. 3. A repeated zone illustration of a Fermi surface slice of V. The slice, which is along the (001) and (010) directions and contains the Γ point, has all the interesting Fermi surface calipers for understanding the oscillatory behavior of the IEC. The calipers are displayed with arrows and labeled with the oscillation periods that they correspond to.

face of V, we find several candidate extremal calipers (see Fig. 3) that could contribute to the coupling oscillations. These would result in the periods 2, 3, 3.5, 4.3, 12, and 20 ML. The results agree fairly well with Ref. 12, where there is a long period oscillation of 20 ML and several short period oscillations in the range 2–5 ML. Three of the calipers in our calculation correspond quite well to periods extracted from the electronic structure calculations.

From the phase diagrams in Fig. 2, we see a gradual change of the coupling periods with increased impurity concentration. All the considered impurities contain more valence electrons than V. The effect of alloying with small amounts of impurities can be seen as an increased electron filling, leading to an expansion of the V electron Fermi surfaces and a reduction of hole Fermi surfaces. Each Cr, Fe, Co, and Ni atom contributes one, three, four, and five extra electrons, respectively. The change in oscillation periods with impurity concentration is, therefore, expected to occur at different rates for the different impurities, where Cr should lead to a rather slow change, whereas Ni should lead to a much more rapid change in the Fermi surface. This is directly seen in the phase diagrams in Fig. 2, where the oscillation fringes of the low concentration region are differently tilted depending on impurity type. In the Fermi surface analysis, the periods of the 4.3 and 12 ML oscillations are expected to increase, while the 3 and 20 ML period oscillations are expected to decrease. The 3.5 and 2 ML periods should remain fairly unchanged.

Generally, we also expect a phase shift of the coupling, which has a complex dependence on both the Fermi surface and the reflection asymmetry at the interfaces but, due to the limited number of spacer thicknesses in our calculations, it is difficult to extract any information about this phase change. There may also be small effects on the amplitude of the exchange coupling as function of alloying due to increased

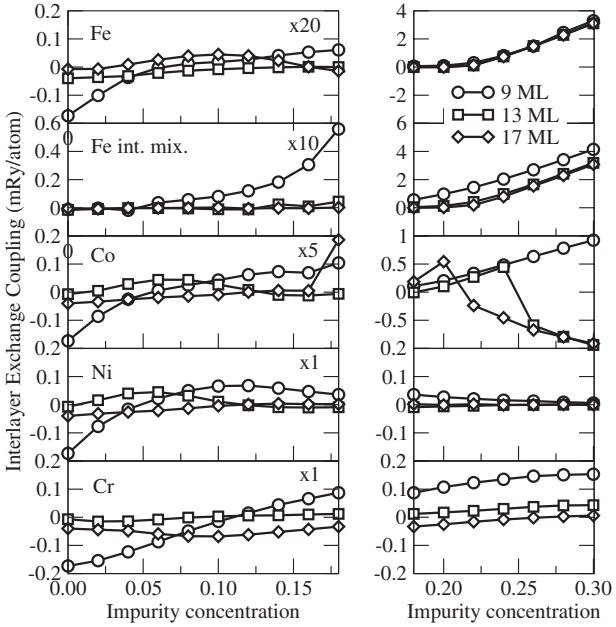

FIG. 4. The graphs show the IEC for multilayers with spacer impurities of Fe, Fe (with interface intermixing $\Gamma_C=1.8$, see Ref. 5), Co, Ni, and Cr. For each graph, we present the coupling for three spacer thicknesses: 9, 12, and 17 ML. On the right hand side, we show the high impurity region ($0.18<x\leq 0.30$) and, on the left hand side, we show the low impurity region ($0.00\leq x\leq 0.18$) in a blown up scale.

or decreased nesting areas on the Fermi surface[21] and from changing magnetic susceptibilities.[22]

2. Disorder damping

A damping of the coupling amplitude due to disorder scattering in the spacer according to Eq. (2) is also expected. Some examples of the damping are indirectly illustrated in Fig. 4, where we have plotted the IEC directly for a few thicknesses. A damping of the amplitude is best seen for the case of Ni impurities, but is also present in the low impurity region for Fe and Co impurities. For Ni impurities, we see a general weakening of the coupling strength with increasing impurity concentration and the amplitude is significantly damped already at impurity concentrations of 20%.

B. Direct exchange region

The onset of magnetism in the spacer is, to a large extent, determined by the concentration, at which there is an onset of magnetism in the bulk. By looking at the V spacer in pure Fe/V multilayers, the electronic structure of V is strongly perturbed compared to the bulk electronic structure for the atoms close to the Fe interface. This results in a V moment at the interface that is antiparallel to the Fe moment. In Fig. 5, we present the magnetization profiles of the spacer for Fe/Fe_xV_{1-x} multilayers in FM alignment of the Fe layers. Data are presented for 9 and 17 ML spacers and for two choices of x in the transition zone between the low and high impurity concentration regions.

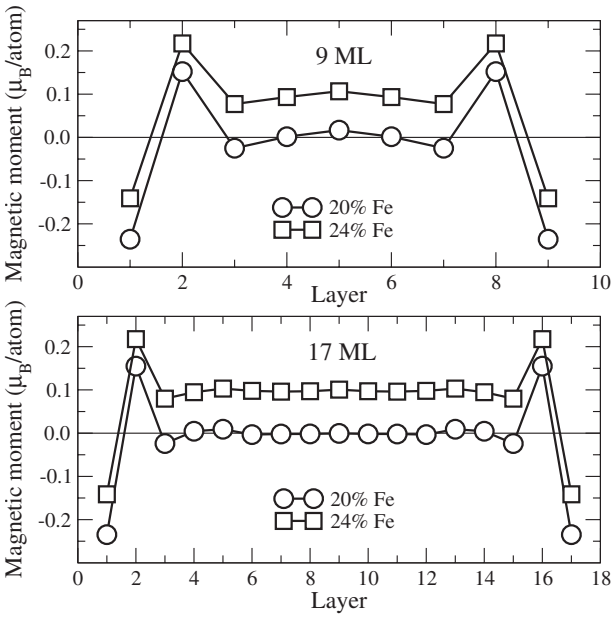

FIG. 5. Profiles of the magnetic moment for the spacers of $Fe/[Fe_xV_{1-x}]$ multilayers in a FM arrangement of the magnetic layers for two choices of spacer thicknesses, 9 and 17 ML, and for two choices of impurity concentrations, 20% and 24% Fe.

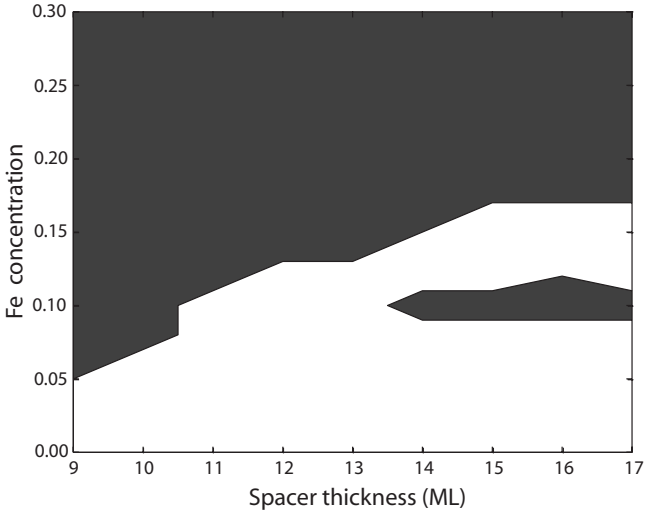

FIG. 6. Phase diagram for $Fe_3/[Fe_xV_{1-x}]_n$ including the effect of intermixing (Γ_c=1.8, see Ref. 5). The horizontal axis shows the spacer thicknesses n and the vertical axis shows the impurity concentration x in the spacers. Black regions represent FM ordering and white regions represent AFM ordering.

For x=0.24, where the IEC is FM for all thicknesses, the center of the spacer is found to be ferromagnetic, while for x=0.20, where the IEC still has some AFM regions, the center is found to have a total magnetization close to zero for both 9 and 17 ML. The transition between nonmagnetic and ferromagnetic spacers lies between these two values of the Fe impurity concentration. Note that the transition concentration was found to be insensitive to the spacer thickness. This fact is also illustrated in Fig. 4, where the sudden increase in the IEC takes place at the same concentration for different spacer thicknesses.

It is interesting to note that for the case of Fe impurities, the coupling switches to strongly FM coupling at almost the same concentration for all spacer thicknesses, whereas if some intermixing is introduced at the interfaces, this behavior is changed (Fig. 4).

We have found that the location of the RKKY and direct exchange regions in the phase diagrams strongly depends on the impurity type. The onset of the direct exchange region occurs at the onset of magnetism in the spacer, which can be estimated from the bulk calculations in Fig. 1. For both Fe and Co, the bulk onset occurs at 20%, which explains the boundary in the multilayers at around 18%. For Ni, the onset of magnetism occurs at 80% Ni and, hence, the investigated range is purely in the low concentration region. For the Cr/V alloy spacers, a comparison with bulk calculations is more difficult since the alloys may exhibit spin-density waves and antiferromagnetic order in the bulk state that can manifest themselves differently in a multilayer.[23] A complete investigation of the complex magnetic structures of $Fe/Cr_xV_{1-x}/Fe$ multilayers is a tremendous task and is beyond the scope of this paper.

C. Influence of interface structure

For modeling an interface structure, we use the same approach as in our previous work,[4,5] where interface intermixing and interface roughness were modeled by two parameters that specify the extent of mixing and roughness. In Fig. 6, we present a phase diagram for Fe/Fe_xV_{1-x} that includes only the effect of interface intermixing. The effects of roughness on the interlayer coupling are thought to be less pronounced in these systems due to the high degree of alloying in the spacer and are not taken into account in this study. Interface intermixing results in an overall damping of the coupling because of the reduced reflection at the interfaces. There is also a reduction in the Fe magnetic moment due to the increased hybridization with V and, consequently, the magnetic thickness of the Fe layers is decreased. Such hybridization has been theoretically[24] observed in Fe/V multilayers.

On the other hand, when more Fe is introduced in the spacer as the impurity concentration is increased, the effective magnetic thickness may increase under certain circumstances. This effect was not seen to have any consequence for the coupling in multilayers with perfect interfaces, but in realistic multilayers with interface intermixing, the effect is seen. For example, by comparing panels 1 and 2 in Fig. 4, it is possible to see that the onset of FM coupling due to direct exchange is earlier for thinner spacer layers in the case of intermixed interfaces. The Fe concentration close to the Fe interface is higher than the average Fe impurity concentration of the spacer, and the interface region reaches the threshold concentration for onset of magnetism before the average impurity concentration reaches this threshold. The magnetic layers are effectively larger by this effect, leading to an effective shrinking of the spacer which, in turn, modifies the RKKY coupling. This results in an additional modification of the coupling and may explain why the whole change in

oscillation period with increasing impurity concentration is not accounted for by changing Fermi surface calipers.

IV. SUMMARY

For low concentrations, all the considered impurities are nonmagnetic in the V host. Varying the impurity concentration within the low concentration region results in a slight change of the coupling periods by modifying the spacer Fermi surface. For larger impurity concentrations, the opening of a channel for direct exchange distorts this picture. For Fe, and to some extent Co, this leads to a ferromagnetic coupling between the layers. For Co, there is also an AFM region for thick spacer layers with high impurity concentrations. For Ni and Cr impurities, the atoms remain nonmagnetic for the whole investigated concentration range (up to 30% impurity concentration). We also discuss the effects of interface intermixing and interface roughness on the phase diagram of Fe/V_xFe_{1-x}. These effects were modeled by using the methods presented in Refs. 5, 18, and 25. In summary, the phase diagram can be understood as consisting of two regions, a low impurity region and a high impurity region. In the low concentration region, the coupling is given by the RKKY coupling. The onset of magnetism in the spacer for higher concentrations eventually leads to a direct exchange mediated coupling between the Fe layers. The onset of magnetism in the spacer exhibits preasymptotic effects, which affect the RKKY coupling.

ACKNOWLEDGMENTS

Financial and facility support from the Swedish Foundation for Strategic Research (SSF), the Swedish Research Council (VR), the Royal Swedish Academy of Sciences (KVA), and the National Super Computer centers (NSC and HPC2N) is acknowledged. B.S. wishes to acknowledge NGSSC. E.H. is grateful to the support from TBC. Valuable discussions with B. Hjörvarsson are acknowledged.

[1] S. A. Wolf, D. D. Awschalom, R. A. Buhrman, J. M. Daughton, S. von Molnár, M. L. Roukes, A. Y. Chtchelkanova, and D. M. Treger, Science **294**, 1488 (2001).
[2] A. Barthélémy, A. Fert, J.-P. Contour, M. Bowen, V. Cros, J. M. De Teresa, A. Hamzic, J. C. Faini, J. M. George, J. Grollier, F. Montaignea, F. Paillouxa, F. Petroffa and C. Vouille, J. Magn. Magn. Mater. **242-245**, 68 (2002).
[3] G. A. Prinz, Science **282**, 1660 (1998).
[4] B. Skubic, E. Holmström, D. Iusan, O. Bengone, O. Eriksson, R. Brucas, B. Hjörvarsson, V. Stanciu, and P. Nordblad, Phys. Rev. Lett. **96**, 057205 (2006).
[5] E. Holmström, L. Nordström, L. Bergqvist, B. Skubic, B. Hjörvarsson, I. A. Abrikosov, P. Svedlindh, and O. Eriksson, Proc. Natl. Acad. Sci. U.S.A. **101**, 4742 (2004).
[6] H. L. Skriver and N. M. Rosengaard, Phys. Rev. B **43**, 9538 (1991).
[7] J. P. Perdew, K. Burke, and M. Ernzerhof, Phys. Rev. Lett. **77**, 3865 (1996).
[8] B. Wenzien, J. Kudrnovský, V. Drchal, and M. Sob, J. Phys.: Condens. Matter **1**, 9893 (1989).
[9] P. Soven, Phys. Rev. **156**, 809 (1967).
[10] I. A. Abrikosov and H. L. Skriver, Phys. Rev. B **47**, 16532 (1993).
[11] B. L. Gyorffy, Phys. Rev. B **5**, 2382 (1972).
[12] M. D. Stiles, Phys. Rev. B **48**, 7238 (1993).
[13] P. Bruno, Phys. Rev. B **52**, 411 (1995).
[14] J. Kudrnovský, V. Drchal, P. Bruno, I. Turek, and P. Weinberger, Phys. Rev. B **54**, R3738 (1996).
[15] P. Bruno, J. Kudrnovský, V. Drchal, and I. Turek, J. Magn. Magn. Mater. **165**, 128 (1997).
[16] N. N. Lathiotakis, B. L. Györffy, E. Bruno, and B. Ginatempo, Phys. Rev. B **62**, 9005 (2000).
[17] M. van Schilfgaarde and F. Herman, Phys. Rev. Lett. **71**, 1923 (1993).
[18] B. Skubic, E. Holmström, O. Eriksson, A. M. Blixt, G. Andersson, B. Hjörvarsson, and V. Stanciu, Phys. Rev. B **70**, 094421 (2004).
[19] M. M. Schwickert, R. Coehoorn, M. A. Tomaz, E. Mayo, D. Lederman, W. L. O'Brien, T. Lin, and G. R. Harp, Phys. Rev. B **57**, 13681 (1998).
[20] P. Granberg, P. Nordblad, P. Isberg, B. Hjörvarsson, and R. Wäppling, Phys. Rev. B **54**, 1199 (1996).
[21] E. Holmström, A. Bergman, L. Nordström, I. A. Abrikosov, S. B. Dugdale, and B. L. Györffy, Phys. Rev. B **70**, 064408 (2004).
[22] E. Holmström, L. Nordström, and A. M. N. Niklasson, Phys. Rev. B **67**, 184403 (2003).
[23] A. M. N. Niklasson, B. Johansson, and L. Nordström, Phys. Rev. Lett. **82**, 4544 (1999).
[24] O. Le Bacq, B. Johansson, and O. Eriksson, J. Magn. Magn. Mater. **226-230**, 1722 (2001).
[25] E. Holmström, Ph.D. thesis, Uppsala University, 2003.